Generalized procedure to determine the dependence of steady-state photoconductance lifetime on the occupation of multiple defects

Keith R. McIntosh,[1,a)] Bijaya B. Paudyal,[1] and Daniel H. Macdonald[2]
[1]*Centre for Sustainable Energy Systems, Australian National University, Canberra, ACT 0200, Australia*
[2]*Department of Engineering, Australian National University, Canberra, ACT 0200, Australia*

(Received 25 July 2008; accepted 21 August 2008; published online 17 October 2008)

We present a procedure to determine the dependence of photoconductance lifetime on the occupation of multiple defects. The procedure requires numerical iteration, making it more cumbersome than the analytical equations available for single-defect and simplified two-defect cases, but enabling the following features: (i) it accounts for the defect concentration when calculating the equilibrium carrier concentrations, (ii) it permits recombination through any number of defects, (iii) it calculates the occupation fraction of all defects at any injection, and (iv) it promotes a good understanding of the role of defect occupation in photoconductance measurements. The utility of the numerical procedure is demonstrated on an experimental sample containing multiple defects. The dependence of the sample's photoconductance on carrier concentration and temperature can be qualitatively described by the generalized procedure but not by either analytical model. The example also demonstrates that the influence of defect occupation on photoconductance lifetime measurements is mitigated at elevated temperatures—a conclusion of particular worth to the study of multicrystalline silicon. © *2008 American Institute of Physics*. [DOI: 10.1063/1.2999640]

I. INTRODUCTION

Carrier lifetime τ_{eff} is routinely determined by steady-state photoconductance.[1] This technique consists of measuring a sample's excess conductance ΔS as a function of photogeneration G, converting $\Delta S(G)$ to excess carrier concentration by assuming that the excess electron Δn and hole Δp concentrations are equal, and finally, by converting $\Delta n(G)$ to $\tau_{\text{eff}}(\Delta n)$ using the carrier mobility and sample width. The assumption that $\Delta n = \Delta p$ is invalid, however, when a significant fraction of light-generated carriers populates defect states rather than the conduction or valence bands. These carriers are "trapped" and do not contribute to ΔS.

The influence of defect occupation on S was first examined in the mid-1950s by Hornbeck and Haynes[2] and Fan.[3] They described its best known manifestation in which there are two defects: a "recombination defect" that dominates at high carrier concentrations and a "trapping defect" that dominates at lower carrier concentrations. This two-defect trapping is observed in all multicrystalline silicon so much so that in some cases τ_{eff} cannot be measured by photoconductance at illumination levels relevant to photovoltaic operation.[4] Two-defect trapping has also been observed in some monocrystalline silicon.[5,6]

An analytical equation that relates S to the occupation of a single defect has been derived by Blakemore.[7] The single defect's occupation has a subtle influence on S and τ_{eff} that might easily go unnoticed. An expression for the defect concentration above which Blakemore's equation is required (i.e., when Δn is significantly different from Δp) is derived by Macdonald and Cuevas[8] and extended by Yashin[9] to remove a restriction on the permissible $\Delta n/\Delta p$ ratio. Yashin accounted for the influence of defect concentration on equilibrium concentrations.[9]

An analytical equation for a two-defect model has also been derived.[2] It is limited, however, by two assumptions: (i) that the population and depopulation of one defect—the trapping defect—are only possible from one band (conduction or valence) and therefore, that no recombination occurs through this defect and (ii) that the defect is entirely unoccupied at equilibrium and entirely occupied under illumination. As such, it cannot account for the temperature dependence of S and τ_{eff}, as described in Sec. III.

In this work, we present a generalized procedure to describe the influence of defect occupation on S and τ_{eff} for any number of defects. It is consistent with Blakemore's equation for a single defect and avoids the long simultaneous equations that result when extending this equation to multiple defects. It is also consistent with the Hornbeck–Haynes model when the aforementioned assumptions are valid. While more complicated than its analytical counterparts, the merits of the procedure are that (i) it accounts for the defect concentration when calculating the equilibrium carrier concentrations, (ii) it permits recombination through any number of defects, (iii) it calculates the occupation fraction of all defects at any injection, and (iv) it promotes a good understanding of the role of defect occupation in photoconductance measurements.

We first present the generalized procedure to numerically determine S and τ_{eff} and then provide an example that demonstrates its utility. The example also illustrates that the debilitating effect of trapping on photoconductance lifetime measurements can be circumvented by raising the sample's

a)Electronic mail: krmcIntosh@gmail.com.

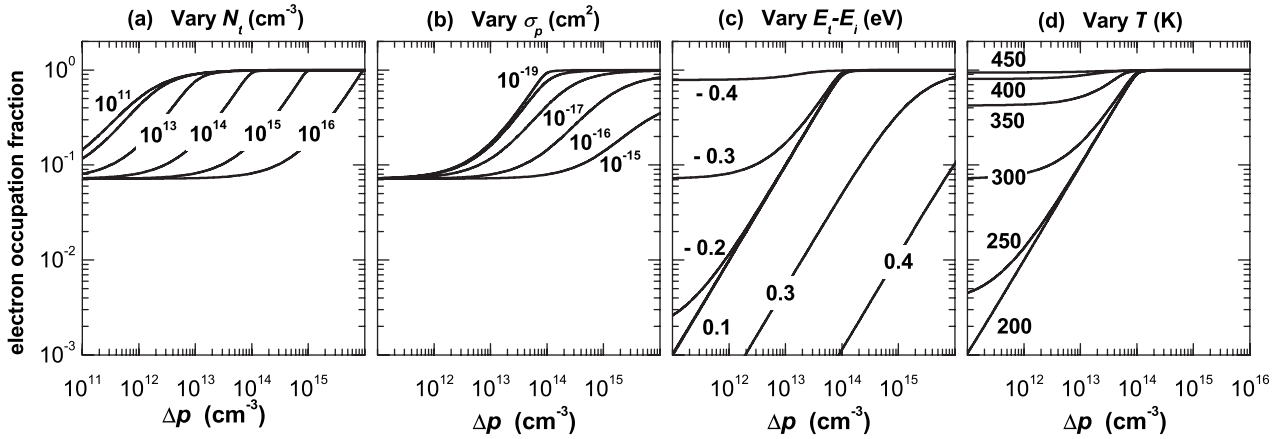

FIG. 1. Electron occupation fraction f_n as a function of excess hole concentration Δp and (a) trap density N_t, (b) electron capture cross section σ_n, (c) defect energy above the intrinsic energy E_t-E_i, and (d) absolute temperature T. Unless noted, the plots are calculated for 1 Ω cm p-type silicon with $N_t=10^{14}$ cm^{-3}, $\sigma_n=10^{-15}$ cm^2, $\sigma_p=10^{-19}$ cm^2, $E_t-E_i=-0.3$ eV, and $T=300$ K.

temperature: at an elevated temperature, the defect occupation remains constant with injection, validating the assumption that $\Delta n=\Delta p$.

II. THEORY

A. General photoconductance lifetime theory

A steady-state photoconductance lifetime measurement involves the comparison of a sample's conductance under photogeneration $S(G)$ to its conductance at equilibrium S_0 (i.e., $G=0$). For all G, S depends on the free electron n and hole p concentrations within the sample, the mobility of those electrons μ_n and holes μ_p, the width of the sample W, and the elementary charge q by the equation

$$S = q\int^{W} (\mu_n n + \mu_p p)dx. \tag{1}$$

Being one dimensional, Eq. (1) assumes spatial uniformity in directions perpendicular to x.

It is usually assumed that the excess electron Δn and hole Δp concentrations induced by the illumination are equal,

$$\Delta n = n - n_0 = p - p_0 = \Delta p, \tag{2}$$

and constant with x so that Eq. (1) simplifies to[10]

$$\Delta S = S - S_0 = q(\mu_n + \mu_p)\Delta n W. \tag{3}$$

Equation (3) also entails the assumptions that ΔS in the surface diffusions (if present) is negligible and that W is constant with G. [When the sample contains either a surface diffusion or surface charge, W represents the width of the quasineutral bulk and can change due to depletion-region modulation (DRM).[11–13]]

Thus, with a measurement of $\Delta S(G)$ and W and with a value for $(\mu_n+\mu_p)$, photoconductance measurements yield $\Delta n(G)$. One can therefore determine the sample's effective lifetime τ_{eff} in steady state $(G=U)$ as defined by[1]

$$\tau_{\text{eff}}(\Delta n) \equiv \frac{\Delta n}{U(\Delta n)}. \tag{4}$$

B. Defect occupation fraction

Equation (2) requires the concentration of defects occupied by electrons n_t and holes p_t to be the same under illumination as at equilibrium. When this is not the case, Δn and Δp are given by

$$\Delta n = (n + n_t) - (n_0 + n_{t0}), \tag{5a}$$

$$\Delta p = (p + p_t) - (p_0 + p_{t0}), \tag{5b}$$

where $n_t=f_nN_t$, $p_t=(1-f_n)N_t$, N_t is the defect concentration, and f_n is the fraction of defects occupied by an electron,[14]

$$f_n = \frac{\sigma_n n + \sigma_p p_1}{\sigma_n(n + n_1) + \sigma_p(p + p_1)}, \tag{6}$$

where σ_n and σ_p are the electron and hole capture cross sections,

$$n_1 = n_i \exp[(E_t - E_i)/kT], \tag{7a}$$

$$p_1 = n_i \exp[(E_i - E_t)/kT], \tag{7b}$$

where E_t is the energy level of the defect, E_i is the intrinsic Fermi level, n_i is the intrinsic carrier concentration, k is the Boltzmann constant, and T is the absolute temperature.

Thus, if f_n is constant for all G, and therefore, for all carrier concentrations, n_t and p_t must also be constant (i.e., equal to n_{t0} and p_{t0}). In this case, Eq. (5) simplifies to Eq. (2) and the theory of the previous section is valid.

There is, however, a variety of conditions for which f_n changes significantly with carrier concentration. Figure 1 provides an example, plotting f_n as function of the excess majority carrier concentration Δp for 1 Ω cm p-type silicon and as a function of (a) N_t, (b) σ_p, (c) E_t-E_i, and (d) T. Except for the featured parameter, the calculations of each plot were made for the baseline parameters: $N_t=10^{14}$ cm^{-3}, $\sigma_n=10^{-15}$ cm^2, $\sigma_p=10^{-19}$ cm^2, $E_t-E_i=-0.3$ eV, and $T=300$ K. Having asymmetrical capture cross sections, a high defect concentration, and a defect energy far from the band edges, these parameters demonstrate how f_n can vary significantly with Δp.

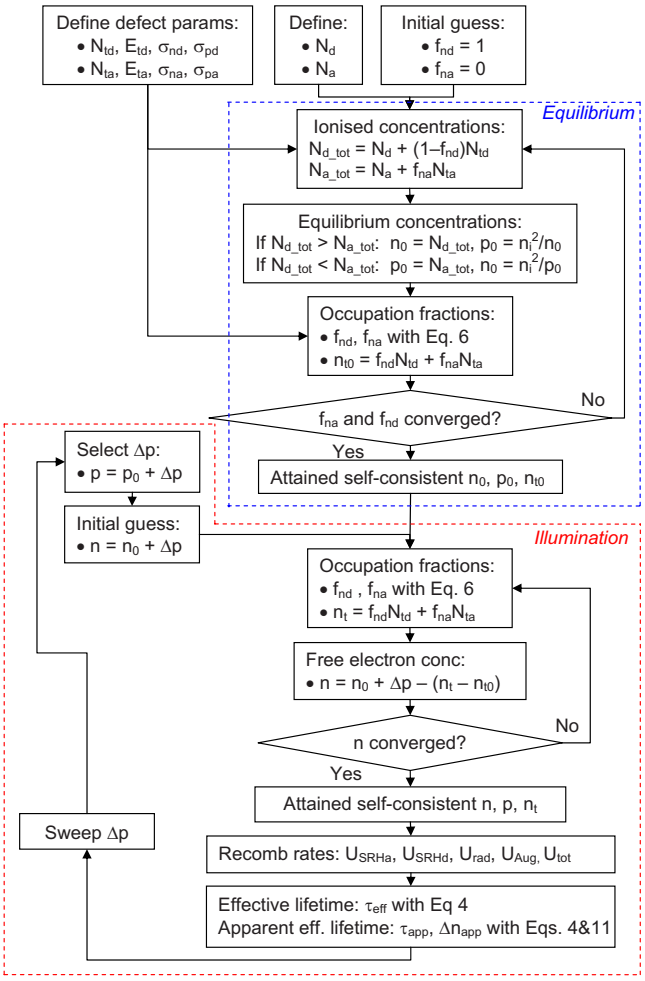

FIG. 2. (Color online) Numerical procedure to determine $f_n(\Delta p)$ and $\tau_{\text{eff app}}(\Delta n_{\text{app}})$.

The most notable features of Fig. 1 are as follows. (a) The excess majority carrier concentration that fully occupies the defect increases with N_t. (b) As the ratio of minority to majority capture cross section increases, the transition from empty to occupied defects occurs more sharply at the point where the excess majority carrier concentration equals N_t. (c) The defect states are fully occupied when E_t lies near the valence band and unoccupied when E_t lies near the conduction band. By contrast, when E_t is nearer midgap, the defects are mostly unoccupied when $\Delta p < N_t$ but fully occupied when $\Delta p > N_t$. (d) At low temperature, the defects are unoccupied when $\Delta p < N_t$ but fully occupied when $\Delta p > N_t$, whereas at high temperature, the defects are fully occupied at all Δp. This final plot demonstrates that f_n at equilibrium is affected by sample temperature—a feature that is exploited in Sec. III.

C. Procedure to account for nonconstant defect occupation

A procedure to determine how defect occupation affects photoconductance lifetime measurements is presented in Fig. 2. This flow diagram is specific to a sample with one donorlike and one acceptorlike defect but is easily adapted to any number of defects of either type.

First, the equilibrium concentrations are determined: n_0, p_0, and n_{t0}. This requires definition of the background dopant concentration for donor N_d and acceptor N_a atoms as well as recombination parameters associated with the donorlike defect (N_{td}, E_{td}, σ_{nd}, and σ_{pd}) and acceptorlike defect (N_{ta}, E_{ta}, σ_{na}, and σ_{pa}). With an initial estimate of the defect occupation fractions f_{nd} and f_{na}, the total number of ionized donor $N_{d\ \text{tot}}$ and acceptor $N_{a\ \text{tot}}$ concentrations can be determined with

$$N_{d\ \text{tot}} = N_d + (1 - f_{nd})N_{td}, \tag{8a}$$

$$N_{a\ \text{tot}} = N_a + f_{na}N_{td}, \tag{8b}$$

where complete ionization of all donor and acceptor atoms is assumed (although it is also possible to treat them as defects with their own energy levels instead).

If $N_{d\ \text{tot}} > N_{a\ \text{tot}}$, the sample is n-type and $n_0 = N_{d\ \text{tot}}$ and $p_0 = n_i^2/n_0$, or if $N_{d\ \text{tot}} < N_{a\ \text{tot}}$, the sample is p-type and $p_0 = N_{a\ \text{tot}}$ and $n_0 = n_i^2/p_0$. With n_0 and p_0, the new values of f_{nd} and f_{na} are calculated with Eq. (6), and iteration of the above steps gives a self-consistent solution to n_0, p_0, and n_{t0}, where

$$n_{t0} = f_{nd}N_{td} + f_{na}N_{ta}. \tag{9}$$

Once the equilibrium concentrations have been attained, steady-state illumination concentrations can be determined by a slightly different approach. The simplest method is to solve for n, p, and n_t at a given value of Δp (or equivalently, Δn). Initial values for n and p are chosen to be $n = n_0 + \Delta p$ and $p = p_0 + \Delta p$. f_{nd} and f_{na} can then be calculated with Eq. (6) to give

$$n = n_0 + \Delta p - (n_t - n_{t0}) \tag{10a}$$

and

$$p = p_0 + \Delta p + (n_t - n_{t0}), \tag{10b}$$

where $n_t = f_{nd}N_{td} + f_{na}N_{ta}$. Iterating Eqs. (6) and 10 to attain convergence provides self-consistent values for n, p, and n_t and therefore for Δn and Δp using Eq. (5).

Once the carrier concentrations are known, it is possible to calculate the Shockley–Read–Hall recombination rate through each defect, as well as Auger and radiative recombination rates.[15] By summing these components (and therefore assuming no carrier hopping between defects), one attains the total recombination rate U as a function of either Δn or Δp and therefore τ_{eff}.

Finally, the photoconductance S can be determined as a function of U (equal to G in steady state) from the free carrier concentrations and Eqs. (1) or (3). Importantly, $S(G)$ is what is determined by experimental photoconductance measurements.

D. Apparent lifetime

In photoconductance experiments, one rarely has knowledge of the dominating recombination parameters (N_t, E_t, σ_n, and σ_p). In such a case, it is impossible to calculate f_n and separate values for Δn and Δp. Instead, one assumes $\Delta n = \Delta p$ [Eq. (2)] to determine the *apparent* effective lifetime $\tau_{\text{eff app}}$ rather than the actual effective lifetime τ_{eff}. This is

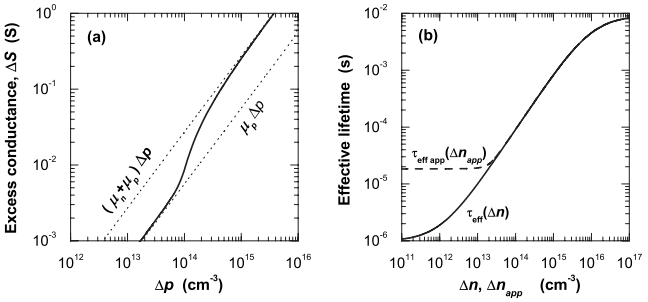

FIG. 3. (a) Excess conductance and (b) effective and apparent lifetimes calculated for the baseline conditions of Fig. 1. Note that the transition due to f_n approaching unity occurs at $\Delta p \sim N_t$, or equivalently, at $\Delta n_{\text{app}} \sim N_t \mu_p/(\mu_n+\mu_p)$.

achieved using the apparent excess carrier concentration Δn_{app},

$$\Delta n_{\text{app}} = \frac{\Delta S}{q(\mu_n + \mu_p)W}, \tag{11}$$

and substituting Δn_{app} into Eq. (4) to find $\tau_{\text{eff app}}$. [Almost all work published on photoconductance measurements made this assumption and therefore presented $\tau_{\text{eff app}}(\Delta n_{\text{app}})$ rather than $\tau_{\text{eff}}(\Delta n)$.] Thus, with the application of Eqs. (11) and (4), the generalized procedure can also determine $\tau_{\text{eff}}(\Delta n)$ and $\tau_{\text{eff app}}(\Delta n_{\text{app}})$ for any set of defect parameters.

E. Deviation in apparent from actual lifetime for a single defect

Figure 3 provides an example of how $\tau_{\text{eff app}}$ can deviate from τ_{eff} for a single defect. It plots (a) $\Delta S(\Delta p)$ and (b) $\tau_{\text{eff app}}(\Delta n_{\text{app}})$ and $\tau_{\text{eff}}(\Delta n)$ for the baseline parameters in Fig. 1. Under sufficient illumination, ΔS is proportional to $(\mu_n + \mu_p)\Delta p$ (Eq. (3)) because all defects are occupied and the excess carrier concentrations are much greater than the defect concentration. In this case, Eq. (2) is valid and $\tau_{\text{eff app}}$ equals τ_{eff}. Under low illumination, however, ΔS is proportional to $\mu_p \Delta p$ because all light-generated electrons occupy the defect rather than the conduction band and do not contribute to the conductance. In this case, there are no additional free electrons to recombine and U is constant with Δp. Thus, while one can plot $\tau_{\text{eff app}}(\Delta n_{\text{app}})$ at low Δn_{app}, no data have actually been taken at Δn lower than when $\tau_{\text{eff app}}$ deviates from τ_{eff}. In practice, it is difficult to know when this has occurred.

The relationship between $\tau_{\text{eff app}}(\Delta n_{\text{app}})$ and $\tau_{\text{eff}}(\Delta n)$ can be assessed using the generalized procedure, but it can also be examined explicitly using Blakemore's model for a single defect.[7–9] Macdonald and Cuevas[8] and Yashin[9] derived expressions that state the conditions under which N_t causes a deviation in $\tau_{\text{eff app}}(\Delta n_{\text{app}})$ from $\tau_{\text{eff}}(\Delta n)$ and they described the trends between $\tau_{\text{eff app}}$ and τ_{eff} as a function of Δn, N_t, E_t, and σ_n/σ_p. These dependencies are complicated but can be summarized for silicon at room temperature to state that $\tau_{\text{eff app}}$ deviates from τ_{eff} when the following conditions are met: (i) the minority capture cross section is significantly larger than the majority capture cross section, (ii) E_t is not near either band edge, and (iii) $\Delta n < N_t$.

It is noteworthy that the deviation in $\tau_{\text{eff app}}(\Delta n_{\text{app}})$ from $\tau_{\text{eff}}(\Delta n)$ due to a single defect is subtle, and to the authors' knowledge, it has not been observed experimentally. With modern instrumentation, however, this might be achieved by the comparison of photoluminescence and photoconductance measurements.

F. Deviation in apparent from actual lifetime for two defects

The most easily observable experiment in which a varying f_n can be detected is through photoconductance measurements of multicrystalline silicon.[4,16–19] In some cases, $\tau_{\text{eff app}}(\Delta n_{\text{app}})$ deviates so greatly from $\tau_{\text{eff}}(\Delta n)$ that it prevents any room-temperature assessment of recombination. Dubbed photoconductance "trapping," this artifact, which manifests as a sharp rise in $\tau_{\text{eff app}}(\Delta n_{\text{app}})$ with decreasing Δn_{app}, cannot be explained with a single defect but requires the existence of two defects: a "recombination" defect and a trapping defect.[2]

Figure 4 illustrates the effect of trapping, plotting

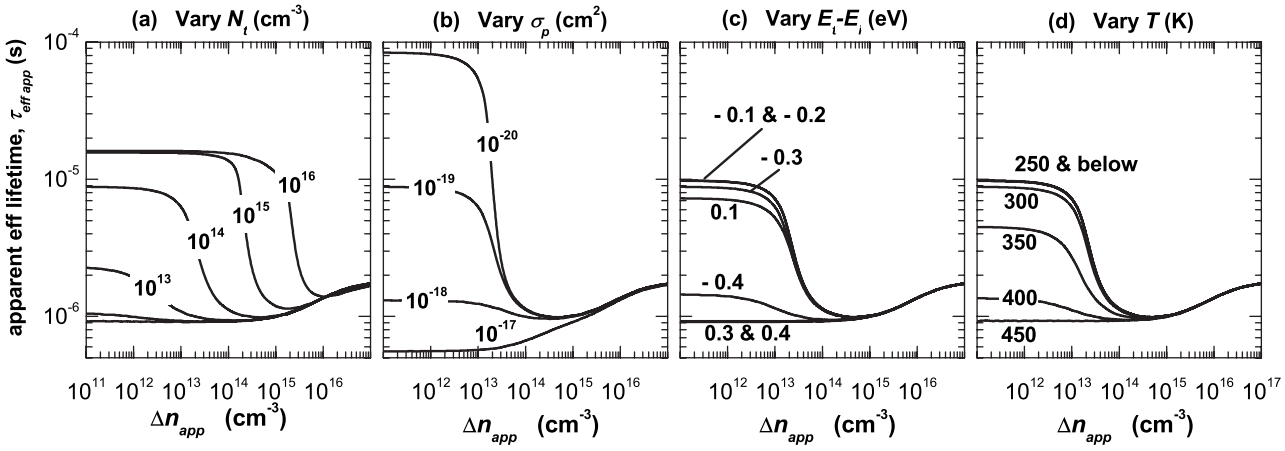

FIG. 4. Apparent effective lifetime $\tau_{\text{eff app}}$ as a function of apparent excess electron concentration Δn_{app} for 1 Ω cm p-type silicon with two defects at 300 K. The first defect has $N_t = 10^{14}$ cm^{-3}, $\sigma_n = \sigma_p = 10^{-15}$ cm^2, and $E_t - E_i = 0$ eV and the second defect has $N_t = 10^{14}$ cm^{-3}, $\sigma_n = 10^{-15}$ cm^2, $\sigma_p = 10^{-19}$ cm^2, and $E_t - E_i = -0.3$ eV. The figure plots the dependence of $\tau_{\text{eff app}}(\Delta n_{\text{app}})$ on the second defect's (a) trap density N_t, (b) electron capture cross section σ_n, and (c) defect energy above the intrinsic energy $E_t - E_i$ as well as (d) the absolute temperature T.

$\tau_{\text{eff app}}(\Delta n_{\text{app}})$ for 1 Ω cm p-type at 300 K. These curves were determined by the generalized procedure for two donor-like defects, where one defect is at midgap with symmetrical capture cross sections, defined with $N_t=10^{14}$ cm^{-3}, $\sigma_n=\sigma_p=10^{-15}$ cm^2, and $E_t-E_i=0$ eV, and where the second trapping defect has the same parameters as those used in Fig. 1. (To permit a simple comparison between curves, the calculations omit intrinsic recombination and the temperature dependence of mobility and thermal velocity and capture cross section. It is trivial to include such effects in the generalized procedure if the dependencies are known.)

The role of the trapping defect is evident in Fig. 4. As injection decreases, there is a sudden rise in $\tau_{\text{eff app}}$, which saturates at a value higher than the actual τ_{eff}. As for a single defect, the saturation results from the recombination being limited by a lack of minority carriers, which populate defects rather than the conduction or valence bands.

Other pertinent features of Fig. 4 are as follows. (a) The sharp rise in $\tau_{\text{eff app}}$ occurs at higher Δn_{app} as N_t increases. (b) The saturation level of $\tau_{\text{eff app}}$ increases as the majority carrier capture cross section of the trapping defect decreases. (c) The deviation in $\tau_{\text{eff app}}$ from τ_{eff} does not occur when the trapping defect is near either band edge because f_n is constant. (d) The deviation in $\tau_{\text{eff app}}$ from τ_{eff} is greatest at low T when f_n of the trapping defect is zero at equilibrium, whereas $\tau_{\text{eff app}}$ does not deviate from τ_{eff} at high T because f_n is unity at all injection. These conclusions are consistent with those for Fig. 1, which plots f_n of the trapping defect.

Prior to this work, the effect of two-defect occupation on photoconductance lifetime had been assessed with the Hornbeck–Haynes model.[2,4,6,20,21] This model assumes that f_n of the trapping defect switches from unity to zero under illumination and does not permit recombination (i.e., either σ_n or σ_p equals 0). It has the advantage of generating an explicit equation to account for trapping on a photoconductance lifetime curve, but it does not permit a detailed assessment of all parameters as performed here. Most notably, it cannot account for changes in f_n due to temperature—a relationship that is now exploited experimentally.

III. EXPERIMENT

The deviation in $\tau_{\text{eff app}}$ from τ_{eff} is sometimes considered a reason to avoid photoconductance measurements of multicrystalline silicon,[22] and as evident in Fig. 4, the deviation can be vast. Figure 4(d) illustrates, however, that the deviation in $\tau_{\text{eff app}}$ from τ_{eff} is increasingly suppressed with increasing temperature. Photoconductance measurements at elevated temperature therefore provide a means to circumvent the influence of multicrystalline trapping. Temperature-controlled measurements also permit a more detailed characterization of the defects.

Figure 5 provides an example of temperature-controlled photoconductance lifetime measurements of a 290 μm thick 1 Ω cm p-type multicrystalline silicon wafer. A low surface recombination velocity was attained by coating the surfaces with amorphous silicon nitride by plasma-enhanced chemical vapor deposition (PECVD),[15] thereby preventing surface recombination from affecting the measurements.

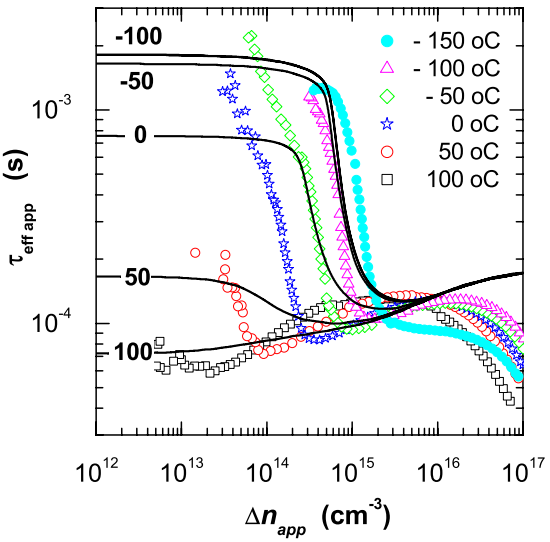

FIG. 5. (Color online) $\tau_{\text{eff app}}(\Delta n_{\text{app}})$ for 1 Ω cm p-type multicrystalline silicon wafer for a range of sample temperatures. The symbols represent experimental points and for clarity, only every fourth point is plotted. The lines were calculated with the generalized procedure for two defects: the first defined by $N_t=10^{13}$ cm^{-3}, $\sigma_n=\sigma_p=10^{-16}$ cm^2, and $E_t-E_i=0$ eV and the second by $N_t=3\times10^{15}$ cm^{-3}, $\sigma_n=10^{-17}$ cm^2, $\sigma_p=10^{-21}$ cm^2, and $E_t-E_i=-0.4$ eV.

The experimental data (symbols) were taken using an apparatus described in Ref. 23. It exhibits the aforementioned trend of a sudden increase in $\tau_{\text{eff app}}$ with decreasing Δn_{app} at some onset concentration Δn_{onset} as well as a decrease in Δn_{onset} with increasing T. In this example, Δn_{onset} is less than 10^{13} cm^{-3} at 100 °C, which is sufficiently low to analyze τ_{eff} at almost all meaningful injection levels. It is interesting that Δn_{onset} does not saturate with decreasing temperature, indicating that the trapping defects are not entirely populated—even at the low temperature of −150 °C. At high Δn_{app}, $\tau_{\text{eff app}}$ decreases rapidly due to Auger recombination. Finally, while there is a faint suggestion that $\tau_{\text{eff app}}$ might saturate with decreasing Δn_{app} at lower temperatures, $\tau_{\text{eff app}}$ continues to rise monotonically. This disagreement between theory and experiment is likely due to the existence of additional trapping defects.

The experimental data of Fig. 5 cannot be modeled by either Blakemore's equation for a single defect, which cannot produce a sudden rise in $\tau_{\text{eff app}}$, or by Hornbeck and Haynes's equation for two defects, which does not reduce Δn_{onset} with temperature. The trends in the data do, however, agree reasonably with those determined by the generalized procedure for two defects—as illustrated by the lines in Fig. 5. The curves were generated for a recombination defect at midgap with symmetric capture cross sections and defined by $N_t=10^{13}$ cm^{-3}, $\sigma_n=\sigma_p=10^{-16}$ cm^2, and $E_t-E_i=0$ eV, and a trapping defect below midgap with asymmetric capture cross sections and defined by $N_t=3\times10^{15}$ cm^{-3}, $\sigma_n=10^{-17}$ cm^2, $\sigma_p=10^{-21}$ cm^2, and $E_t-E_i=-0.4$ eV. The resulting theoretical trends agree reasonably with the experimental trends, but no attempt was made to optimize the fit between theory and experiment. Since the capture cross sections and even the defect level can change with temperature and since a variety of defects is expected to exist in the impurity laden grain boundaries, attaining high agreement

between theory and experiment would require the fine tuning of an impractical number of parameters. What can be concluded from the simulation is that the multicrystalline silicon is reasonably well modeled as having a high concentration of defects ($\sim 2 \times 10^{15}$ cm^{-3}) with an energy in the lower half of the bandgap and with σ_n much smaller than σ_p.

We note that the experimental data were not influenced by transient effects, as construed from varying the illumination decay constant and attaining identical results. We do not ascribe the increase in $\tau_{\text{eff app}}$ to DRM because the samples did not contain a *p-n* junction[12,13] and because following the procedure in Ref. 11, the charge density in the PECVD silicon nitride (at most 5×10^{12} cm^{-2}) (Ref. 15) is insufficient to cause an increase in $\tau_{\text{eff app}}$ at a Δn near or above Δn_{onset}.

IV. CONCLUSION

This work presented a numerical procedure to determine a semiconductor's apparent and actual lifetimes accounting for the occupation of any number of defects. An experimental example that illustrated the utility of the procedure was provided. The example also showed that the detrimental influence of trapping in multicrystalline silicon can be mitigated by performing photoconductance measurements at elevated temperature.

ACKNOWLEDGMENTS

We thank Bruce Condon for his assistance with the temperature-controlled measurements and Bart Geerligs from the Energy Research Centre of the Netherlands (ECN) for supplying the experimental sample. This work was funded by an Australian Research Council Linkage Grant between the Australian National University, SierraTherm Production Furnaces, and SunPower Corporation. D.M. is supported by an Australian Research Council fellowship.

[1] R. A. Sinton and A. Cuevas, Appl. Phys. Lett. **69**, 2510 (1996).
[2] J. A. Hornbeck and J. R. Haynes, Phys. Rev. **97**, 311 (1955).
[3] H. Y. Fan, Phys. Rev. **92**, 1424 (1953).
[4] D. Macdonald and A. Cuevas, Appl. Phys. Lett. **74**, 1710 (1999).
[5] D. Macdonald, M. Kerr, and A. Cuevas, Appl. Phys. Lett. **75**, 1571 (1999).
[6] J. Schmidt, K. Bothe, and R. Hezel, Appl. Phys. Lett. **80**, 4395 (2002).
[7] J. S. Blakemore, *Semiconductor Statistics* (Pergamon, Oxford, 1962), Sec. 8.4.
[8] D. Macdonald and A. Cuevas, Phys. Rev. B **67**, 075203 (2003).
[9] A. N. Yashin, Semiconductors **39**, 1285 (2005).
[10] D. E. Kane and R. M. Swanson, in *Measurement of the Emitter Saturation Current by a Contactless Photoconductivity Decay Method*, Proceedings of the 18th IEEE Photovoltaics Specialist Conference, Las Vegas, 1985 (IEEE, New York, 1985), p. 578.
[11] M. Bail, M. Schulz, and R. Brendel, Appl. Phys. Lett. **82**, 757 (2003).
[12] P. J. Cousins, D. H. Neuhaus, and J. E. Cotter, J. Appl. Phys. **95**, 1854 (2004).
[13] K. R. McIntosh, IEEE Trans. Electron Devices **54**, 346 (2007).
[14] W. Shockley and W. T. Read, Phys. Rev. **87**, 835 (1952).
[15] A. G. Aberle, *Crystalline Silicon Solar Cells: Advanced Surface Passivation and Analysis* (University of New South Wales, Sydney, 1999).
[16] V. Yelundur, A. Rohatgi, J. W. Jeong, and J. I. Hanoka, IEEE Trans. Electron Devices **49**, 1405 (2002).
[17] H. F. W. Dekkers, L. Carnel, and G. Beaucarne, Appl. Phys. Lett. **89**, 013508 (2006).
[18] M. C. Schubert and W. Warta, Prog. Photovoltaics **15**, 331 (2007).
[19] M. Dhamrin, C. Schmiga, K. Kamisako, and T. Saitoh, Sol. Energy Mater. Sol. Cells **90**, 3179 (2006).
[20] M. C. Schubert, S. Riepe, S. Bermejo, and W. Warta, J. Appl. Phys. **99**, 114908 (2006).
[21] P. Pohl, J. Schmidt, K. Bothe, and R. Brendel, Appl. Phys. Lett. **87**, 142104 (2005).
[22] R. A. Bardos, T. Trupke, M. C. Schubert, and T. Roth, Appl. Phys. Lett. **88**, 053504 (2006).
[23] B. B. Paudyal, K. R. McIntosh, D. H. Macdonald, B. S. Richards, and R. A. Sinton, Prog. Photovoltaics **16**, 609 (2008).